IEEE Robotics and Automation Letters (RAL) paper presented at the
2020 IEEE/RSJ International Conference on Intelligent Robots and Systems (IROS)
October 25-29, 2020, Las Vegas, NV, USA (Virtual)

R-Track: Separable Modular Climbing Robot Design for Wall-to-Wall Transition*

Changmin Park[1], Jangho Bae[2], Sijun Ryu[1], Jiseok Lee[1], and TaeWon Seo[1], *Senior Member, IEEE*

***Abstract*— This paper presents the development of a reconfigurable wall-climbing robot (WCR) called R-track. R-Track is designed for operations inside metal structures. It adheres to the metal surface with magnetic tracks. With a modular design which each module of R-Track can be connected or disconnected without an additional actuator, R-Track can perform various wall-to-wall transitions. In particular, external wall transitions that have been difficult for previous WCRs can be achieved by R-track with a cooperation between modules. The statics of R-Track during wall transitions was analyzed to identify and verify an appropriate reconfiguration strategy. Experiments on wall-to-wall transitions were conducted to demonstrate the performance of R-Track. The results indicate that R-Track successfully performed all kinds of perpendicular wall-to-wall transitions.**

I. Introduction

Wall-climbing robots (WCR) have been researched for performing tasks on vertical spaces. One of the main tasks of WCRs on the vertical spaces is an inspection of dangerous and complicated structures. The main requirements of inspection task are mobility and velocity [1]. For the thorough inspection of the structures, mobility is more important than velocity. WCRs must not only be able to adhere on a vertical wall during operations, but also be capable of three-dimensional (3D) motions, which include transitions between two surfaces, i.e., wall-to-wall transitions, because the structures tend to have many walls connected with sharp edges. Several locomotion methods were developed to make a WCR move on the vertical surfaces.

The most straightforward idea is to tie a rope at the top of the structure and make the robot move through it, but it has a limited workspace. Seo et al. installed a rope ascender in the robotic platform and developed a façade cleaning system that can overcome obstacles of the limited size on the vertical wall [2]. The next idea is step-based locomotion, which uses legs or prismatic joints to move on the surface step by step. Step-based WCRs mainly use legs whose feet have the adhesive force toward a vertical wall. There are many step-based WCRs, but many of them can only perform planar walking on a single wall [3]–[5]. To perform a wall-to-wall transition, a WCR should have many degrees of freedom (DOF) or compliance on its legs. For example, Anyclimb designed by Liu et al. can move on curved walls using a compliant walking mechanism with a dry adhesive footpad [6]. Still, this is not adequate for inspecting complicated structures.

WCRs using tracks can perform a wall-to-wall transition more easily than step-based WCRs. Therefore, researches on tracked WCRs are more focused on 3D motions on the surface, including wall-to-wall transitions. Shen et al. designed a WCR with permanent magnet tracks that could overcome obstacles on the single wall [7]. MultiTrack having tracks with suction cups could perform over-the-thin-wall tasks because of its high maneuverability, but did not show wall-to-wall motion [8]. Unver and Sitti developed the Tankbot, with tracks made of adhesive material, to realize wall-to-wall transitions and steering, but only internal wall-to-wall transitions could be achieved [9]. External wall-to-wall transitions are harder than internal wall-to-wall transitions. Lee et al. proposed a magnetic track robot that can realize a 90° vertical wall-to-wall transition, covering one each of internal and external wall-to-wall transitions [10]. They improved their designs and developed Combot, which can perform more difficult wall-to- wall transitions at various angles [11], [12]. However, any robot to the best of our knowledge could not succeed ceiling to wall external transition, which is the most difficult wall-to-wall transition.

Modular design and reconfiguration can be a solution to perform the ceiling to wall external transition. A modular mobile robot can move across various environments by changing the connection between its modules. Hirose et al. proposed "Gunryu" system, which can change its module connection [13]. They demonstrated the concept of movement across a cliff and step obstacle by the reconfiguration of the system. Spröwitz et al. developed "Roombots," a modular robotic system using an active connector mechanism [14]. Roombots can perform wall-to-wall transitions limitedly on walls having connectors for attachment. Casarez and Fearing developed a stair-climbing legged robot that contains two identical modules [15]. The modules are connected when climbing a step obstacle, which is impossible for one module. Similar to this work, Seo and Sitti developed MultiTank, which uses a dry adhesive track mechanism [16]. MultiTank has two modules and can perform a wall-to-wall transitioning and an over-the-thin-wall task. These studies show that modular design and reconfiguration let robotic systems deal with challenging terrains.

In this study, we designed and fabricated a separable modular WCR called "R-Track." R-Track consists of three

*This work was supported by the Basic Science Research Program through the National Research Foundation (NRF) of Korea funded by the Ministry of Science, ICT (NRF-2017R1A2B4002123). (*Corresponding author: TaeWon Seo*) (*Co-first authors: Changmin Park and Jangho Bae*)

[1]C. Park, S. Ryu, J. Lee, and T. Seo are with the School of Mechanical Engineering, Hanyang University, Seoul, 04763, Korea pcm900530@gmail.com; fbtlwns007@gmail.com; jisuk500@gmail.com; taewonseo@hanyang.ac.kr

[2]J. Bae is with GRASP Laboratory, University of Pennsylvania, Philadelphia PA 19104, United States jangho.bae91@gmail.com

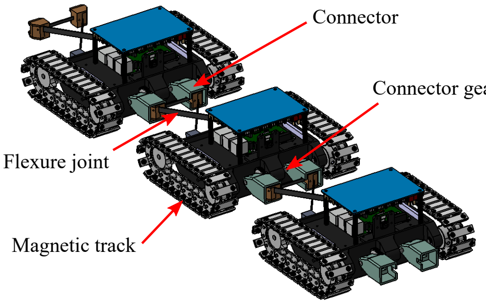

Fig. 1. 3D drawing of the three R-Track modules.

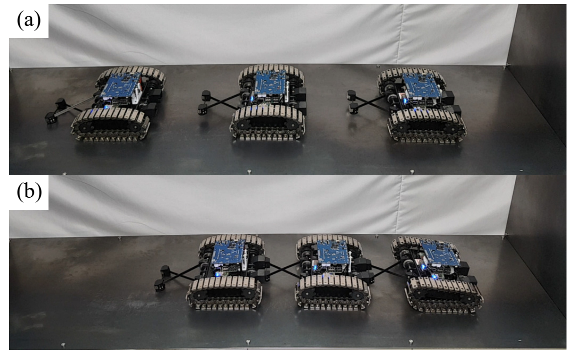

Fig. 2. Connection and disconnection of R-Track modules: (a) fully-separated modules; (b) fully-connected R-Track.

separable modules equipped with permanent magnetic tracks. Each module can operate separately and independently. Through attachment and detachment of modules, the system can transit between two adjacent surfaces with high stability. The main contributions of this study are as follows.

- We designed and fabricated a modular WCR, R-Track.
- We developed a locomotion strategy for all internal and external wall-to-wall transitions, including ceiling to wall external transition, which has not been done with other WCRs.
- We explored possibility of the locomotion strategy by static analysis.
- We proved the performance of R-Track with experiments.

The remainder of this paper is organized as follows. In Section II, the design and configuration of R-track are presented. The reconfiguration strategy and static analysis for wall-to-wall transitions is explained in Section III. The experimental results are presented and discussed in Section IV. Finally, the conclusions are summarized in Section V.

II. System Design

A. R-Track Design

R-Track was designed for climbing ferromagnetic surfaces with magnetic tracks. The primary feature of R-Track is its modular design, which enables all wall-to-wall transitions. R-Track consists of three identical modules as presented in Fig. 1. Each module consists of the main body, magnetic tracks, and the actuated tail. The main body containing electrical parts, such as battery and motor drivers, is made of AL6061 and 3D-printed parts.

N35-grade neodymium magnet pieces were used to create the magnetic tracks. One piece of magnet (34.8 mm $\times$ 9.5 mm $\times$ 3 mm) can apply 10.6 N of stiction force to a steel wall. By using neodymium magnets, one module can climb a vertical steel wall with an additional 2 kg payload. To render the module steerable, two magnetic tracks are used on each side for locomotion. Each magnetic track is actuated independently by an electric motor (XM430-W350-R, Robotiz, Korea).

The connector, which also uses neodymium magnets, was designed to attach and detach without using an additional actuator. The male connector is placed at the end of the tail, whereas the female connector is placed at the front. The modules can detach themselves by creating a velocity difference between them with the traction force from the magnetic tracks. To attach two modules, the horizontal position is matched by movement of the modules, whereas the vertical position is matched by adjusting the height of the tail. The shape of the connector helps correct a certain amount of position error. Fig. 2 details the connection and disconnection of the R-Track modules.

For successful wall-to-wall transition, the system must maintain positive normal forces. Therefore, we designed the tail of the module actuated with an electric motor (XM430-W350-R, Robotiz, Korea). By applying torque to the tail, the reaction force from the surface is applied on the tail. This reaction can increase the normal force of the front contact point. Made of carbon fiber for reduced weight and sufficient strength, the tail is designed to be flexible in the horizontal direction but stiff in the vertical direction. Thus, the tail can reduce the elastic reaction force from horizontal steering while applying a force on the wall.

Open-source controller boards (OpenCR1.0, Robotiz, Korea) were used for control each module. The modules are connected to the main controller using Bluetooth (BT410, Robotiz, Korea). Control commands are delivered from a personal computer to each module via Bluetooth signals.

B. Terminology and Dimensions

The structure of the R-Track module can be simplified, as shown in Fig. 3. The main body and tracks are considered as one body. $\boldsymbol{P}_f^i$ denotes the position of the front sprocket of the i-th module, and $\boldsymbol{P}_r^i$ denotes the position of the rear sprocket of the i-th module. The tail is simplified as a linkage connected to the center of the rear sprocket, $\boldsymbol{P}_r^i$. When two modules are connected, the tail is connected to the center of the front sprocket of the other module. Because of the design and positions of the electronic components, the center of mass (COM) of the module is further behind the geometric center of the main body. The position of COM of the i-th module is expressed as $\boldsymbol{CM}^i$. Finally, the angle between the ground and R-Track is denoted as α.

The dimensions of each component are summarized in Fig. 3 and Table I. The sprocket radius is denoted as R, whereas

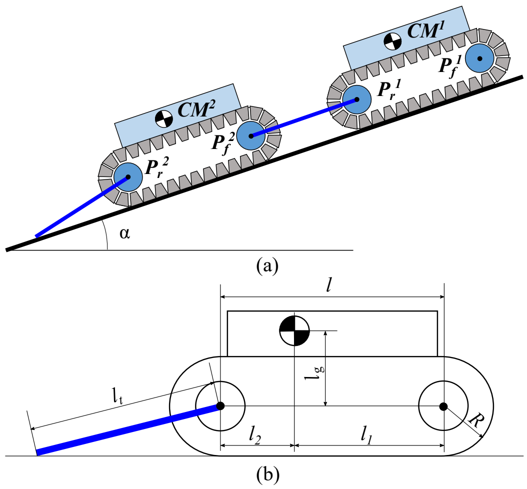

Fig. 3. Simplified kinematic diagram of R-Track module: (a) the two modules connected on the sloped surface; (b) the dimension terminology of R-Track.

the length between two sprocket centers is denoted as l. l_1 and l_2 are the distances between the COM and two sprocket centers. The length of the tail is denoted as l_t. The distance between the COM and centerline of the track is denoted as l_g.

TABLE I
DIMENSIONS OF R-TRACK

R	l	l_1	l_2	l_t	l_g
19.5 mm	139 mm	85.4 mm	53.6 mm	106 mm	30mm

III. STATIC ANALYSIS

A. Problem Definition

We focused on the transitioning between perpendicular walls. Therefore, we only considered walls with slope angles of 0°, 90°, 180°, and 270°. Fig. 4 illustrates all possible transitions between two perpendicular walls and notations of the walls. The wall with 0° slope angle is denoted as wall A. Wall B is the wall with 90° slope angle. The walls with 180° and 270° slope angles are denoted as walls C and D, respectively.

The wall-to-wall transition can be divided into two parts. The internal transition occurs inside the wall structure toward the direction of increasing slope angle: A→B, B→C, C→D, and D→A. On the other hand, the external transition occurs outside the structure toward the direction of decreasing slope angle: A→D, D→C, C→B, and B→A.

B. Internal Wall-to-Wall Transition

The statics of the system was analyzed to prove the possibility of internal wall-to-wall transitions. Fig. 5 details the forces and torque applied to one R-Track module during an internal transition. The subscripts f and r indicate the applied point of each force: f for the front contact point and r for the rear contact point. $\boldsymbol{F_M}$ denotes the magnetic adhesive force between tracks and steel walls. Normal forces from the walls are denoted as $\boldsymbol{F_N}$, and friction forces are expressed as $\boldsymbol{F_f}$. $m\boldsymbol{g}$ is a gravitational term for the weight of the module. The reaction from the active tail is applied to the center of the rear sprocket as torque τ_t.

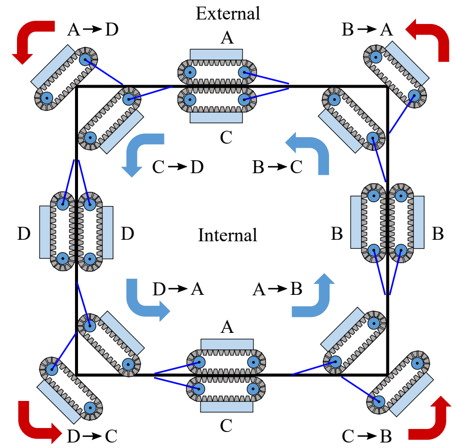

Fig. 4. All possible transitions between two perpendicular walls.

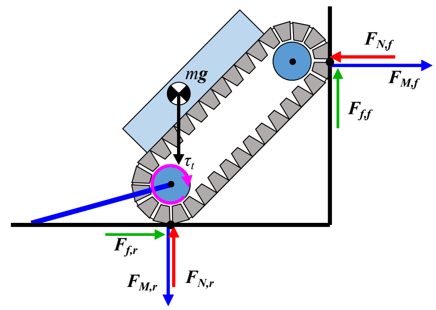

Fig. 5. The force and torque equilibrium of one module transitioning from A to B.

The system was assumed to maintain force and torque equilibrium. Under this assumption, the normal and frictional forces were calculated by solving three equilibrium equations. The magnetic adhesive forces were calculated from the strength of the magnet pieces. In the case of internal transition, two magnetic pieces were stuck to the wall at each contact point, which indicates a magnetic force of 21.2 N for each piece. The force and torque equilibrium equations are as follows:

$$\boldsymbol{F_{N,f}} + \boldsymbol{F_{f,f}} + \boldsymbol{F_{N,r}} + \boldsymbol{F_{f,r}} = -\boldsymbol{F_{M,f}} - \boldsymbol{F_{M,r}} - m\boldsymbol{g}, \quad (1)$$

$$\begin{aligned}(\boldsymbol{C_f} - \boldsymbol{C_r}) \times (\boldsymbol{F_{N,f}} + \boldsymbol{F_{f,f}} + \boldsymbol{F_{M,r}})\\ +(\boldsymbol{CM} - \boldsymbol{C_r}) \times m\boldsymbol{g} + \tau_t = \boldsymbol{0},\end{aligned} \quad (2)$$

where $\boldsymbol{C_f}$ and $\boldsymbol{C_r}$ are the positions of the front and rear contact points of the tracks. The directions of variables can be determined from the wall slope angle. The directions of the normal forces ($\boldsymbol{F_{N,f}}$, $\boldsymbol{F_{N,r}}$) are perpendicular to the contacted wall. Similarly, the directions of the friction forces ($\boldsymbol{F_{f,f}}$, $\boldsymbol{F_{f,r}}$) are parallel to the contacted wall. Therefore,

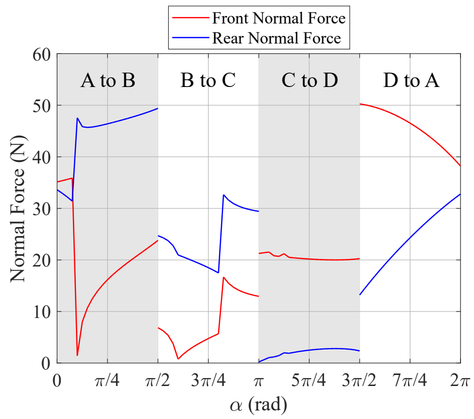

Fig. 6. Normal forces of two contact points during internal transition. The tail torque was set as 0.5 Nm.

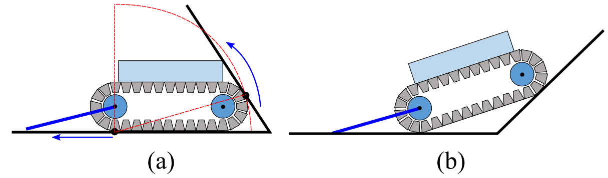

Fig. 7. Non-perpendicular internal wall-to-wall transition: (a) acute angle; (b)obtuse angle.

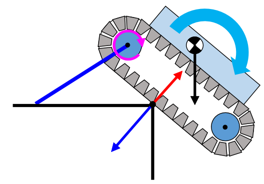

Fig. 8. Tip-over problem caused in external transition with only one module.

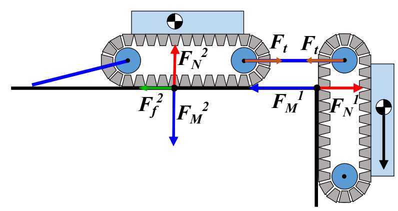

Fig. 9. Solving tip-over problem by connecting two modules.

equilibrium equations have four unknown variables, the magnitudes of normal forces and friction forces.

The solution of (1) and (2) is indeterminate, because the number of variables is larger than that of equations. We selected the determination criterion that minimizes the maximum ratio between the normal and friction forces [17]. After that, we used the optimization solver to find a single solution for the normal and friction forces. The criterion can be summarized as follows:

$$\begin{aligned} &\min_{\boldsymbol{F}} \ \max\left(\frac{|\boldsymbol{F_{f,f}}|}{|\boldsymbol{F_{N,f}}|}, \frac{|\boldsymbol{F_{f,r}}|}{|\boldsymbol{F_{N,r}}|}\right) \\ &\text{subject to } |\boldsymbol{F_{f,f}}| \leq \mu_s |\boldsymbol{F_{N,f}}| \\ &\qquad\qquad\ |\boldsymbol{F_{f,r}}| \leq \mu_s |\boldsymbol{F_{N,r}}| \end{aligned} \tag{3}$$

where μ_s is the maximum static friction coefficient, measured as 0.74, in the previous section. The solution is presented on Fig. 6, which presents the normal force data during internal transitions. Sudden jumps in data were caused by COM position movement, which changes the direction of the friction force. We can conclude that internal transitions can be achieved with one module because the normal forces can be maintained as positive. Moreover, if carefully controlled, internal transitions can be performed with any number of modules.

In addition, R-Track can perform wall-to-wall transition on non-perpendicular walls. If the angle is acute angle, the rear sprocket should move backward during transition. In this case, R-Track cannot perform transition without slip, because the front and rear sprocket is connected with a track and rotate together. However, if angle between two walls is obtuse angle, the transition is easier than doing on perpendicular walls. Two cases of non-perpendicular transition is presented on Fig. 7.

C. External Wall-to-Wall Transition

In the case of external transitions, cooperation between modules is necessary. With one module, the system cannot avoid tip-over at the corner. The problem of one module at the external corner is presented in Fig. 8. When the COM of the module goes over an external edge, the net moment of the system cannot be zero. The system only makes contact with a single point, which means that the magnetic adhesive force cannot produce the moment in the opposite direction. Moreover, the tail can only generate a reaction torque toward the tip-over direction.

The tip-over problem can be avoided by connecting two modules. The simplest case is the external transition from A to D. As shown in Fig. 9, the rear module can provide a supporting force to the front module. The supporting force must be large enough to withstand the moment due to gravity but smaller than the maximum horizontal force that the rear module can hold. The required magnitude of the supporting force under the harshest condition, i.e., right before completing the transition from D to A can be derived as follows:

$$RF_t = (l_g + R)mg, \tag{4}$$

where F_t is the tension, and mg is the gravity. The maximum feasible tension can be calculated as follows:

$$F_t \leq \mu_s (F_m^2 + mg), \tag{5}$$

where μ_s is the maximum static friction coefficient. F_m^2 is the rear module's magnetic force, which is 148.6 N, because 14 magnet pieces were attached to the surface. The maximum feasible tension is 130.3 N, which is higher than the required magnitude, 69.8 N. Therefore, the A to D external transition can be achieved by two modules.

Similar to the A to D external transition, two modules are required to perform D to C and B to A external transitions. The static analysis diagram of the two cases are presented in

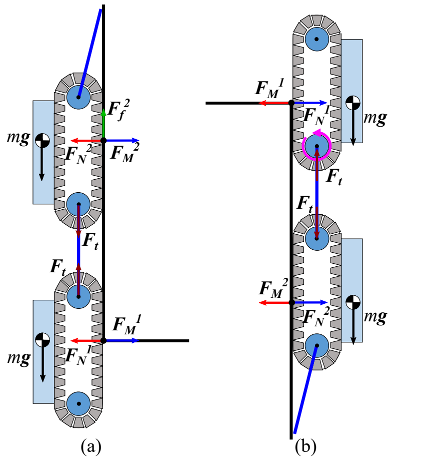

Fig. 10. Static analysis of external wall-to-wall transition: (a)D to C transition; (b) B to A transition.

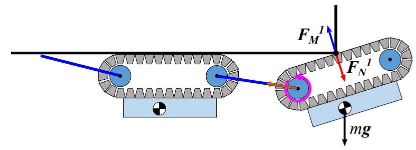

Fig. 11. Achieve C to B external transition by connecting two modules.

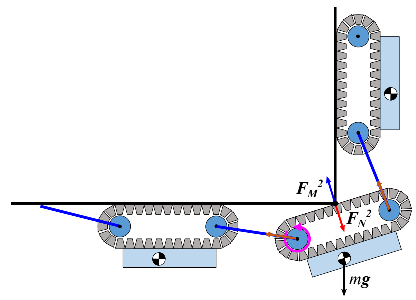

Fig. 12. Achieve C to B external transition by connecting three modules.

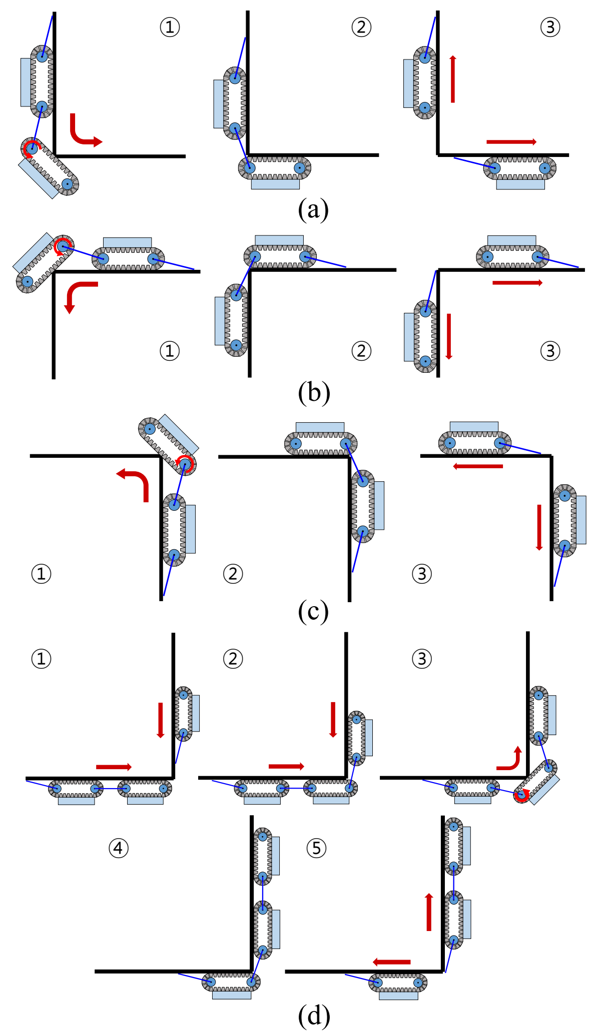

Fig. 13. The transition strategy by using two and three modules: (a) D→C; (b) A→D; (c) B→A; (d) C→B.

Fig. 10. In the case of D to C external transition, the tension force through the tail $\boldsymbol{F_t}$ can support the front module. We calculated the required maximum tension when the front module is attached to the wall with one magnetic piece. As shown in Fig. 10 (a), the required maximum tension force can be calculated as same as (4). The tension is restricted to maintain stiction of the rear module as follows:

$$F_t \leq \mu_s F_m^2 - mg, \tag{6}$$

The required supporting force is 69.8 N, which is lower than the maximum possible magnitude of the force, 82.3 N. The case of the transition from B to A is detailed in Fig. 10. The static analysis of B to A transition is same as equations (4) and (6).

However, when transitioning from C to B, two modules are not enough. Fig. 11 presents a situation where the front module is dangling with one magnet piece. During external transition, the magnetic adhesive force of one magnet, $\boldsymbol{F_M^1}$, is 10.6 N, which is less than the gravitational force, $m\boldsymbol{g}$, is 27.5 N. Because there are no other supporting forces, the front module is unable to maintain the positive normal force, and it shall fall. If there is an additional module on the B side, then the module can be supported through the tail connector, as illustrated in Fig. 12. The maximum possible support force through the tail is $\mu_s|\boldsymbol{F_N^1}| = 104$ N. Therefore, the wall-to-wall transitioning from C to B can only be achieved with three modules.

Same as internal transitions, R-Track can perform external wall-to-wall transitions when two walls make an obtuse angle. In case of acute-angled transition, the transition is much harder than perpendicular transition. However, the obtuse-angled transition is easier, because the front module doesn't need to be go the hardest position as analyzed in this study. Moreover, R-Track can perform side wall-to-wall transitions, because the gravity is not applied against the direction of the front module rotation.

With these results, the wall-to-wall transitioning strategy can be established. Internal transitions can be performed with any number of modules, which means that they do not

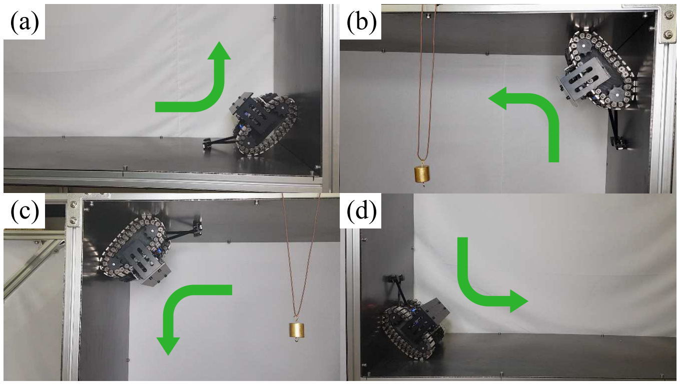

Fig. 14. Performing internal transitions with one R-Track module: (a) A→B; (b) B→C; (c) C→D; (d) D→A. See multimedia extension for details

need any specific method. For external transitions, except for the C to B transition, two modules are required. The key transitioning strategy is completing the transition with two modules and separate modules after it. For the external transition from C to B, three modules are required. The modules on walls B and C pull-up one module on C. The transitioning strategy for external walls is detailed in Fig. 13. By adding more modules, R-Track can conduct multiple wall-to-wall transitions consecutively. Therefore, R-Track can inspect more complicated structure with additional modules.

IV. Experiments

The wall-to-wall transitions of R-Track were demonstrated experimentally. A test bench was built to conduct experiments for all possible transitions. We attached steel plates to the frame of aluminum profiles to create eight corners. All modules were controlled manually by the Bluetooth signals from the control program. We used current control for the tail motors to apply force to the ground, and position control for the sprocket motors.

R-Track could achieve all internal transitions in all configurations. As proved in Section III B, R-Track can perform internal transitions with one module, which means that this can be achieved with any number of modules. The internal wall-to-wall transitions were done by simple control. R-Track successfully performed all internal transitions with one, two, or three modules, as presented on Fig. 14 and the supplementary video.

External transitions were also tested with the proposed transition strategies. The external transitions, except for the transition from C to B, could be achieved with two or three modules. Fig. 15 details the experiments on external transitions with two modules. The C to B external transition, which requires at least three modules, was also performed on the test bench. The transition process with three modules is presented in Fig. 16. Full experimental videos are included in the supplementary material.

The time for finishing transitions are summarized in Table II. Unlike internal transitions, external transitions needed longer time because of attaching and detaching process. Also,

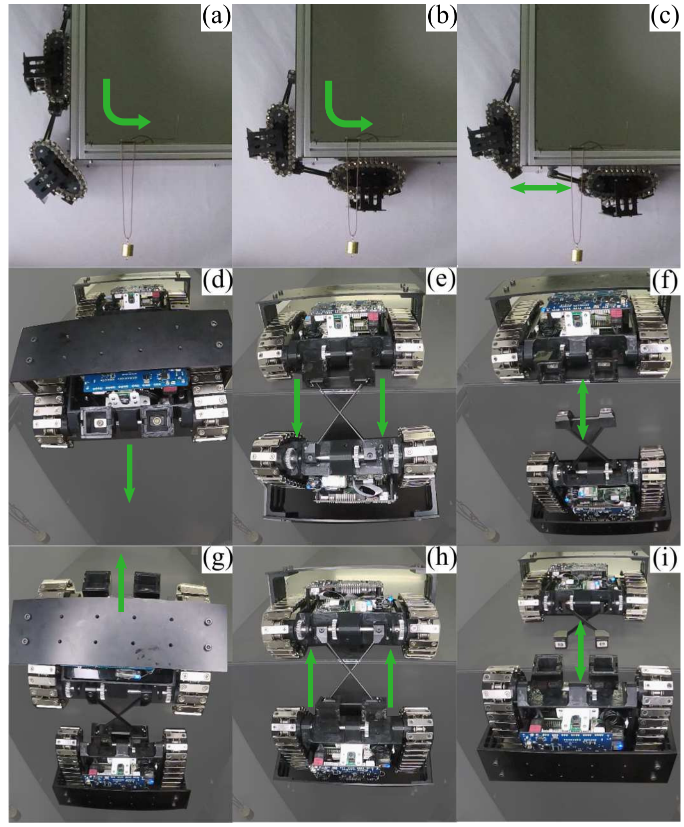

Fig. 15. Performing external transitions with two R-Track modules: (a-c) D→C; (d-f) A→D; (g-i) B→A. See the supplementary video for details.

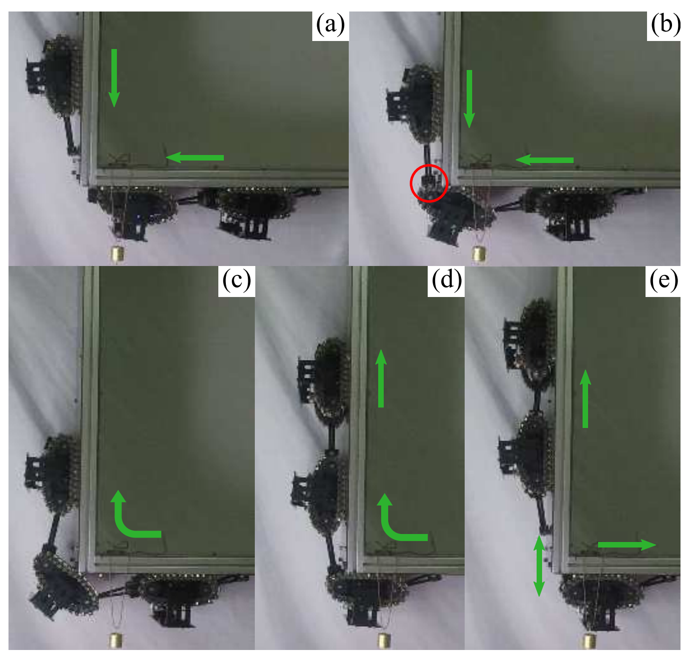

Fig. 16. Experiment on external transition from C to B with three modules. See the supplementary video for details.

the limitation of manual control affected external transition time. This can be improved by developing automated controller for R-Track, which will use normal force and orientation data of each module.

TABLE II

TIME FOR WALL-TO-WALL TRANSITION

Internal	External (2 modules)			External (3 modules)
(1 module)	A→D	D→C	B→A	C→B
3.33 s	25.25 s	31.46 s	32.83 s	52.14 s

V. CONCLUSION

In this study, the reconfigurable WCR, R-Track, was designed and fabricated. R-Track consists of three modules, which can connect or disconnect with each other. With two magnetic tracks, each module can move along metal walls. Through the cooperation between modules, R-Track can perform all kinds of wall-to-wall transitions between perpendicular walls. The reconfiguration strategy was developed by analyzing the statics during each transition. With this strategy, the wall-to-wall transitions of R-Track were verified by experiments on the test bench. In future works, we are planning to develop a torque control algorithm for the R-Track tails. By measuring orientations and normal forces, the proper tail torque can be derived and applied on the tails. Furthermore, a path planning and reconfiguration automation algorithm for inspecting random structures will also be developed.

ACKNOWLEDGMENT

We thank to Youngjoo Lee and Yunhyuk Lee for helping wall-to-wall transition experiments.

REFERENCES

[1] D. Schmidt and K. Berns, “Climbing robots for maintenance and inspections of vertical structures—a survey of design aspects and technologies,” *Robotics and Autonomous Systems*, vol. 61, no. 12, pp. 1288–1305, 2013.

[2] K. Seo, S. Cho, T. Kim, H. S. Kim, and J. Kim, “Design and stability analysis of a novel wall-climbing robotic platform (rope ride),” *Mechanism and Machine Theory*, vol. 70, pp. 189–208, 2013.

[3] B. L. Luk, A. A. Collie, and J. Billingsley, “Robug ii: An intelligent wall climbing robot,” in *Proceedings. 1991 IEEE International Conference on Robotics and Automation*. IEEE, 1991, pp. 2342–2347.

[4] A. Nagakubo and S. Hirose, “Walking and running of the quadruped wall-climbing robot,” in *Proceedings of the 1994 IEEE International Conference on Robotics and Automation*. IEEE, 1994, pp. 1005–1012.

[5] J. C. Grieco, M. Prieto, M. Armada, and P. G. De Santos, “A six-legged climbing robot for high payloads,” in *Proceedings of the 1998 IEEE International Conference on Control Applications (Cat. No. 98CH36104)*, vol. 1. IEEE, 1998, pp. 446–450.

[6] Y. Liu, H. Kim, and T. Seo, “Anyclimb: A new wall-climbing robotic platform for various curvatures,” *IEEE/ASME Transactions on Mechatronics*, vol. 21, no. 4, pp. 1812–1821, 2016.

[7] W. Shen, J. Gu, and Y. Shen, “Proposed wall climbing robot with permanent magnetic tracks for inspecting oil tanks,” in *IEEE International Conference Mechatronics and Automation, 2005*, vol. 4. IEEE, 2005, pp. 2072–2077.

[8] G. Lee, H. Kim, K. Seo, J. Kim, and H. S. Kim, “Multitrack: A multi-linked track robot with suction adhesion for climbing and transition,” *Robotics and Autonomous Systems*, vol. 72, pp. 207–216, 2015.

[9] O. Unver and M. Sitti, “Tankbot: A palm-size, tank-like climbing robot using soft elastomer adhesive treads,” *The International Journal of Robotics Research*, vol. 29, no. 14, pp. 1761–1777, 2010.

[10] G. Lee, K. Seo, S. Lee, J. Park, H. Kim, J. Kim, and T. Seo, “Compliant track-wheeled climbing robot with transitioning ability and high-payload capacity,” in *2011 IEEE International Conference on Robotics and Biomimetics*. IEEE, 2011, pp. 2020–2024.

[11] G. Lee, G. Wu, S. H. Kim, J. Kim, and T. Seo, “Combot: Compliant climbing robotic platform with transitioning capability and payload capacity,” in *2012 IEEE International Conference on Robotics and Automation*. IEEE, 2012, pp. 2737–2742.

[12] G. Lee, G. Wu, J. Kim, and T. Seo, “High-payload climbing and transitioning by compliant locomotion with magnetic adhesion,” *Robotics and Autonomous Systems*, vol. 60, no. 10, pp. 1308–1316, 2012.

[13] S. Hirose, T. Shirasu, and E. F. Fukushima, “Proposal for cooperative robot “Gunryu” composed of autonomous segments,” *Robotics and Autonomous Systems*, vol. 17, no. 1-2, pp. 107–118, 1996.

[14] A. Spröwitz, R. Moeckel, M. Vespignani, S. Bonardi, and A. J. Ijspeert, “Roombots: A hardware perspective on 3d self-reconfiguration and locomotion with a homogeneous modular robot,” *Robotics and Autonomous Systems*, vol. 62, no. 7, pp. 1016–1033, 2014.

[15] C. S. Casarez and R. S. Fearing, “Step climbing cooperation primitives for legged robots with a reversible connection,” in *2016 IEEE International Conference on Robotics and Automation (ICRA)*. IEEE, 2016, pp. 3791–3798.

[16] T. Seo and M. Sitti, “Tank-like module-based climbing robot using passive compliant joints,” *IEEE/ASME Transactions on Mechatronics*, vol. 18, no. 1, pp. 397–408, 2012.

[17] D. Choi, “Development of the rough terrain hybrid mobile robot (rhymo) with low posture variation index and high terrainability,” Ph.D. dissertation, Seoul National University, 2015.